

Setting the Yardstick: A Quantitative Metric for Effectively Measuring Tactile Internet

J.P. Verburg^{*§}, H.J.C. Kroep^{*§}, V. Gokhale^{*}, R. Venkatesha Prasad^{*}, and V. Rao^{*}
^{*}Delft University of Technology, The Netherlands,

Abstract—The next frontier in communications is the *telemanipulation* of remote environments. Compared to conventional network-based applications, telemanipulation poses widely different requirements, which demand a significant redesign of conventional networking techniques as well as their performance metrics. Telemanipulation along with a host of other applications requiring transportation under extremely low latencies is termed as *Tactile Internet* (TI). To support TI, enormous advancements are being made to improve network techniques. On the contrary, performance metrics have barely garnered any research attention. The lack of metrics majorly impedes the overall progress of TI. In this paper, we present our first step towards developing a quantitative metric for TI. We propose a method that characterizes TI in an end-to-end fashion to obtain fine-grained performance in terms of delay and precision. We take Dynamic Time Warping (DTW) as the basis of our work and identify its shortcomings for evaluating TI. To circumvent them, we build upon DTW and propose two new concepts: Effective Time-Offset (ETO) and Effective Value-Offset (EVO). The primary strength of the proposed concepts, together referred to as ETVO, lies in the fact that they can quantitatively characterize the performance of any end-to-end TI system in a manner that is agnostic to underlying implementation details. We present the mathematical framework involved in the design of ETVO. Through rigorous experiments conducted on a realistic TI setup, we compare the performances of DTW and ETVO. Our findings show that ETVO results in $62.5\times$ less time noise for up to 34% increased RMSE compared to DTW.

I. INTRODUCTION

Tactile Internet (TI) [1] is irrefutably at the forefront amid several emerging technological innovations that are foreseen to revolutionize future industries and the lifestyle of humans. The crux of TI is its potential to enable *telemanipulation* - active transportation of physical skills of humans for manipulation and control of remote environments. Sensory feedback, such as audio, video, vibrotactile, and kinesthetic, transmitted via TI, provides a feeling of collocation between geographically distant locations. This feedback facilitates humans to remotely perform activities in uninhabitable or resource-constrained locations as if they are physically present there. Existing studies, such as [2], show that this not only improves the accuracy of the task, but also reduces its execution time significantly. TI will provide massive benefits to the revolution in the manufacturing sector, coupled with Industry 4.0 [3]. A few prominent applications of TI include telesurgery, remote disaster management, immersive VR gaming, and automation.

TI versus current Internet – TI applications are significantly different from the existing real-time applications over

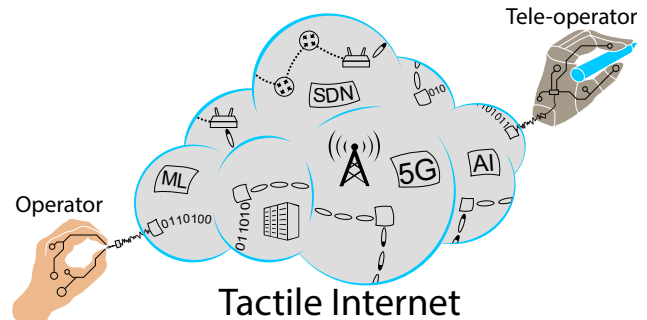


Fig. 1. A high-level representation of the end-to-end TI architecture.

the Internet. For concreteness in exposition, let us take the examples of telesurgery involving audio-video-haptic feedback (TI application) and standard audio-video teleconferencing (real-time Internet application). In the former case, the surgeon's physical actions need to be replicated precisely on the remote patient through a telemanipulator. The resulting physical sensations have to be fed back to the surgeon instantly, which further determines the surgeon's subsequent actions. In this case, it is imperative to not only maintain ultra-low feedback latency (typically sub-10 ms), but also ensure that the telemanipulation is transparent [4], i.e., both precise as well as comfortable to the operator. Non-compliance with any of the above results in severe impairment in the surgeon's ability to operate, potentially leading to catastrophic outcomes. In the latter case with teleconferencing using audio-video, latency in the order of even several hundreds of milliseconds slows the conversation down by a small amount, without hampering the users' ability to interact.

To summarize, for TI applications, not only are the constraints on conventional Quality of Service (QoS) measures, such as latency and reliability, tighter than existing applications but also they are insufficient for design and comprehensive characterization of TI.

State of the art falls short – Thanks to the recent advancements in the field of 5G, particularly in the context of ultra-reliable, low-latency communication (URLLC), TI is enormously benefiting in addressing QoS constraints [5]–[7]. Note that the QoS measures indicate the service quality delivered by TI and are purely quantitative. On the other hand, literature also provides several works that propose utilizing Quality of Experience (QoE) parameters as qualitative measures for TI [8], [9]. Note that the QoE measures indicate

[§]Both authors contributed equally to this work

the user experience of utilizing the TI infrastructure for telemanipulation. A combination of QoS and QoE measures are considered the *de facto* performance indicators of TI. However, a thorough analysis of existing QoS and QoE metrics (presented in Section II) suggests the following.

- Often these metrics lead to contradicting inferences, thereby creating ambiguity in judgment.
- These metrics are usually employed for performance analysis of standalone TI modules. Therefore, it is unclear as to how well they characterize the performance when several TI modules interplay with each other.
- They do not indicate how well a given network solution facilitates applications with feedback.

We provide more insights into the above shortcomings in the state of the art in Sections II and V. The lack of comprehensive performance metrics severely limits the overall progress of TI, which motivates us to take the first step towards bridging this gap.

Our contributions – Our approach is to devise a method that is capable of delineating the fine-grained similarity between the input and output signals of TI in two domains: time and value (amplitude in general). We term the discrepancies between the input and output signals in these two domains, respectively, as *Effective Time-Offset* (ETO) and *Effective Value-Offset* (EVO). Henceforth, for convenience, we call ETO and EVO, and jointly as ETVO. The concept is illustrated in Figure 2, where we treat the entire connection between the operator and the teleoperator as a black box. The advantage of this approach is that the proposed method is robust to the design and implementation of the underlying TI components.

We observe that Dynamic Time Warping (DTW) – a popular scheme for constructing a sample-wise match between two sequences – exhibits several properties that align with our objectives. However, it also manifests significant limitations that prevent it from being directly employed for TI purposes. Hence, we take DTW as a starting point of our design process and carry out substantial refinements through a concrete mathematical framework. In this light, our contributions in this work are broadly summarized as follows:

- We present two novel concepts, *Effective Value-Offset* (EVO) and *Effective Time-Offset* (ETO), that capture fine-grained properties of a TI session, which hitherto was not possible.
- We present a concrete mathematical framework with DTW as a baseline and define these two new concepts to make it suitable for accurate measurement of offsets in a context-aware manner (Section IV).
- We present major drawbacks of DTW itself on why it fails to be a suitable scheme to be used in TI (Section III).
- We design extensive TI experiments consisting of a haptic device, real network setup, and human subjects. We demonstrate the contrast between the inferences drawn by QoE and QoS metrics (Section V).
- We show the efficacy of our scheme in terms of estimating the offsets. Furthermore, we compare them with

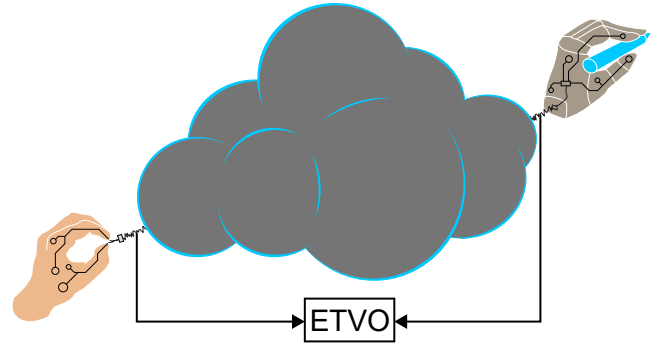


Fig. 2. Our black-box approach for designing a metric considers only the input and output signals as shown in the figure. Our metric is agnostic to all the modules in the grey area.

the performance of DTW (Section V) and illustrate the effects of our refinements.

We believe that the above contributions will act as the basis for more sophisticated designs of metrics for different TI applications under various requirements and constraints.

II. RELATED WORK

A. TI performance metrics

Several QoE and QoS metrics have been devised and extensively used to evaluate TI systems.

1) *QoE*: Subjective QoE metrics, involving users, aim to capture the overall human perception. A few works that adopt this approach include [2], [8]. Haptic Perceptually Weighted Peak Signal to Noise Ratio (HPW-PSNR), as proposed by Sakr et al., incorporates the knowledge of human perception having a logarithmic relationship with the haptic stimulus [10]. Hinterseer et al. presented this idea to measure the PSNR of the reconstructed haptic signal [11]. Continuing this, Chaudhuri et al. proposed Perceptual Mean Square Error (PMSE), which maps MSE to the perceptual domain [9]. A recent work by Hassen et al. proposes the Haptic Structure SIMilarity (HSSIM) index to improve the objective estimation of human perception. HSSIM extends the idea of SSIM, which was initially proposed for images, to haptic signals for computing the similarity between original and reconstructed signals. Hamam et al. took a different approach to analytically model haptic device properties while calculating the objective metric [12].

2) *QoS*: Several modular design validations of TI systems use statistical measures of network characteristics such as packet rate, latency, jitter, and packet losses as QoS metrics. While Admux, an adaptive multiplexer for TI, proposed by Eid et al. uses all of the above metrics [13], the multiplexing scheme by Cizmeci et al. focuses on throughput and latency [14]. Hinterseer et al. proposed a haptic codec that focuses on reducing the overall packet rate [11]. The codec is based on perceptual Deadband, where packets are not sent if the changes are below the level of human perception. The congestion control scheme by Gokhale et al., aims to contain latency and jitter within their permissible limits [15].

B. Signal similarity

An important aspect of TI applications is that the input from the controller should closely match the output at the rendering side, ideally matching each sample. The problem of determining similarity between two time-varying signals has been widely investigated due to their applicability in several domains, for example, speech and gesture recognition. Cross-correlation computes the offset required between the two such that their dot product is maximized [16]. A stationary value is a trivial choice representing the time-varying latency of TI systems. DTW conducts an exhaustive search to achieve sample-wise matching between the two signals in a manner that minimizes the cumulative Euclidean distance [17]. Owing to its popularity, several optimization algorithms for efficient computation of DTW exist, including a few recent ones [18]–[20]. Several follow-up works on DTW exist with each of them attempting to outperform DTW in one or more aspects. The most widely recognized ones include Edit Distance on Real sequences (EDR) [21], Edit distance with Real Penalty (ERP) [22], and Longest Common Sub-Sequence (LCSS) [23]. DTW forms the basis of our metric design.

III. DYNAMIC TIME WARPING AND ITS LIMITATIONS

When a variable delay is involved, the golden standard method for calculating the similarity between two signals is DTW. DTW is heavily used in speech recognition [18]. DTW matches two sequences in time so that the Euclidian distance between individual samples is minimized. In speech recognition this is essential, as it allows DTW to identify the same word spoken at different paces as similar. DTW uses a *warp path*, which indicates a sample-wise mapping between two time-series that minimizes the cumulative Euclidian distance. Figure 3 illustrates two sequences and how DTW matches them.

A. Mathematical description of the DTW algorithm

The accent $\tilde{\cdot}$ indicates mathematical notations specific to DTW. Our proposed solution redefines most variables. We define $\tilde{\mathbf{f}}$ and $\tilde{\mathbf{g}}$ as discrete time series of length N so that $\tilde{\mathbf{f}}, \tilde{\mathbf{g}} \in \mathbb{R}^N$. The DTW algorithm constructs a warp path $\tilde{\mathbf{w}}(\tilde{k}) = (\tilde{\mathbf{w}}_0[\tilde{k}], \tilde{\mathbf{w}}_1[\tilde{k}])$, $\tilde{\mathbf{w}}_0, \tilde{\mathbf{w}}_1 \in \mathbb{N}^{\tilde{K}}$, where the length of the warp path is bound by $N \leq \tilde{K} < 2N$. $\tilde{\mathbf{w}}_0$ and $\tilde{\mathbf{w}}_1$ return the indexes of $\tilde{\mathbf{f}}$ and $\tilde{\mathbf{g}}$, respectively. The warp path represents the matching so that the Cumulative Euclidean distance is minimized.

$$\text{DTW}(\tilde{\mathbf{f}}, \tilde{\mathbf{g}}) = \min_{\tilde{\mathbf{w}}} \sum_{\tilde{k}=0}^{\tilde{K}-1} |\tilde{\mathbf{f}}[\tilde{\mathbf{w}}_0(\tilde{k})] - \tilde{\mathbf{g}}[\tilde{\mathbf{w}}_1(\tilde{k})]|, N \leq \tilde{K} < 2N. \quad (1)$$

The entries in $\tilde{\mathbf{w}}(\tilde{k})$ must meet the following conditions:

1) Monotonicity and continuity:

$$\begin{aligned} \tilde{\mathbf{w}}_0[\tilde{k}] &\leq \tilde{\mathbf{w}}_0[\tilde{k} + 1] \leq \tilde{\mathbf{w}}_0[\tilde{k}] + 1, \\ \tilde{\mathbf{w}}_1[\tilde{k}] &\leq \tilde{\mathbf{w}}_1[\tilde{k} + 1] \leq \tilde{\mathbf{w}}_1[\tilde{k}] + 1. \end{aligned}$$

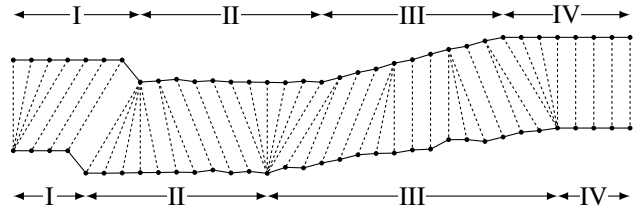


Fig. 3. An illustrative example of how DTW behaves when aligning two signals, the two solid lines indicate two discrete time series and the dashed lines indicate how DTW aligns the samples

2) Boundary:

$$\tilde{\mathbf{w}}(0) = (0, 0) \quad (2)$$

$$\tilde{\mathbf{w}}(\tilde{K} - 1) = (N - 1, N - 1). \quad (3)$$

The computation of $\text{DTW}(\tilde{\mathbf{f}}, \tilde{\mathbf{g}})$ is done two steps.

- 1) Populate a cumulative distance matrix $\tilde{\mathbf{C}} \in \mathbb{R}^{N \times N}$. Every point in this matrix gives a value indicating the cheapest path to that point from the start. Every element is given by,

$$\tilde{\mathbf{C}}[\tilde{i}, \tilde{j}] = |\tilde{\mathbf{f}}[\tilde{i}] - \tilde{\mathbf{g}}[\tilde{j}]| + \min \begin{cases} \tilde{\mathbf{C}}[\tilde{i}, \tilde{j} - 1], \\ \tilde{\mathbf{C}}[\tilde{i} - 1, \tilde{j} - 1], \\ \tilde{\mathbf{C}}[\tilde{i} - 1, \tilde{j}]. \end{cases} \quad (4)$$

- 2) backtrack through $\tilde{\mathbf{C}}$ to construct warp path $\tilde{\mathbf{w}}$, where,

$$\tilde{\mathbf{w}}(\tilde{K} - 1) = (N - 1, N - 1), \text{ and}$$

$$\begin{aligned} \tilde{\mathbf{C}}[\tilde{\mathbf{w}}(\tilde{k} - 1)] &= \min_{\tilde{\mathbf{d}}} \tilde{\mathbf{C}}[\tilde{\mathbf{w}}(\tilde{k}) - \tilde{\mathbf{d}}], \\ \forall \tilde{\mathbf{d}} &\in \{(0, 1), (1, 0), (1, 1)\}. \end{aligned} \quad (5)$$

B. shortcomings of DTW for evaluating TI

DTW is designed for a different purpose, but it provides a method for dealing with time differences and value errors at the same time. This fundamental property makes DTW a suitable starting point. We identify and analyze multiple shortcomings of DTW that make it unsuitable for TI.

1) DTW measures the similarity between two sequences:

DTW, which measures the similarity between two sequences, can be very useful in classifying problems like correlation power analysis, DNA classification, and notably, speech recognition. In the latter, DTW can be used to recognize a word to be the same, even when spoken at different speeds or pitches. In all of these cases, DTW calculates how similar two sequences are, and treats both sequences as equally important. The boundary conditions in Equation (2) and (3), are there to make sure that DTW does not skip any part of either sequence. Figure 3 illustrates an example of DTW. Segments ‘I’ and ‘IV’ show how the boundary conditions lead to start and stop artefacts at the start and end of the sequences.

Instead of calculating how two sequences are similar, we want to calculate how the output is different from the input, where differences due to time or value are distinguished. These

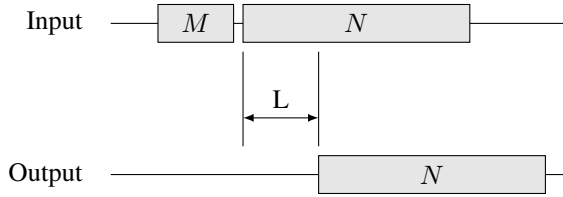


Fig. 4. This figure illustrates how the input and sequence are build up, and how their lengths are chosen

sequences are not symmetrical, as the input is unmodified by definition

2) Delay Adjustments are free in DTW:

The output of DTW is the cumulative Euclidean distance after applying a calculated warp path matching the two sequences. There is a penalty for a change in time because every delay adjustment leads to the inclusion of an extra pair of samples. However, both the delay and delay adjustments are not visible at the output. For applications like speech recognition, this is a desirable property, as differences in delay do not matter when identifying words spoken. However, this is unacceptable for TI, as delay and delay adjustments cause more significant degradation in performance than noise in most cases. Examples are presented in Figure 3. In segment ‘II’, the time derivative of both sequences is low, so that small differences cause large fluctuations in delay. In segment ‘III’, one can see a large number of small changes that lead to minor improvements.

3) DTW pursues the most opportunistic result:

In a pursuit to identify similar sequences, DTW aims for the highest similarity it can find. It has been proven that DTW achieves its goal optimally. As a consequence of this goal, changes to the delay do not have to happen at the moment that causes the change. In most instances, the changes in delay happens earlier. Multiple examples can be found in Figure 3. Segments ‘I’ and ‘IV’ start with an adjustment of delay, even though the changes are made for the end of the segment. At the start of Segment ‘II’ there is a large delay change a few samples before a small peak that causes the change.

We aim for a method that can identify how a system behaves objectively, and not use the best case interpretation.

IV. EFFECTIVE TIME- AND VALUE-OFFSET

We propose two new concepts: Effective Time-Offset (ETO) and Effective Value-Offset (EVO). ETO and EVO are time series, where every sample indicates the time-offset and value-offset of the corresponding output sample respectively. Together ETVO provides fine-grained information on a per-sample basis. The mathematical framework and its reasoning are laid out in three chapters corresponding to the shortcomings outlined in Section III-B.

A. The mathematical foundation of ETVO

As discussed in Section III-B1, there is a fundamental difference between the purpose of DTW and ETVO. The

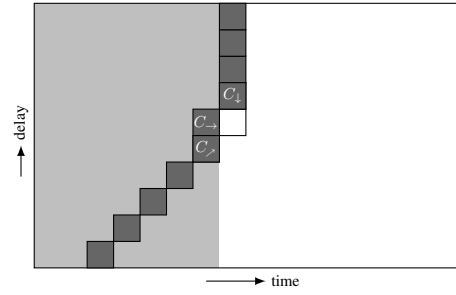


Fig. 5. The squares indicate all the values that need to be considered to calculate the optimum for the value in the white square. Gray indicates that the optimal value for that spot is already calculated. Dark gray indicates the cheapest source to get to the white square for three different methods. These are the only squares that need to be checked

symmetry in DTW is not needed, and the boundary conditions are undesirable. Thus we try to find a different foundation that is better suited for ETVO.

Let $\mathbf{f}[k]$ be a slice of the input, and $\mathbf{g}[k]$ a slice of the output. ETO provides a time-offset to every sample in $\mathbf{g}[k]$ to match it to a sample in $\mathbf{f}[k]$. There is a range of delays that are considered for every sample. The minimum delay is $\Delta T_{min} \in \mathbb{R}$, and the maximum delay is $\Delta T_{max} \equiv \Delta T_{min} + MT$, where $M \in \mathbb{N}^+$, and T the sample period. Let the length of $\mathbf{g}[k]$ be N . To give every sample of $\mathbf{g}[k]$ M possible delays, $\mathbf{f}[k]$ should be of length $N + M - 1$. If the first sample of $\mathbf{g}[k]$ is at $t = 0$, then the first sample of $\mathbf{f}[k]$ should be at $t = -\Delta T_{min} - (M-1)T$. This is illustrated in Figure 4. The warp path is $\mathbf{w} \subset \mathbb{N}^N$, where $w[k]$ indicates that $g[k]$ corresponds to $f[k - w[k]]$. We define the Cumulative Distribution Matrix as $\mathbf{C} \subset \mathbb{R}^{N \times M}$, where the x -axis indicates the sample index of $\mathbf{g}[k]$, and the y -axis the delay of that sample. This is illustrated in Figure 5. The value at each entry of \mathbf{C} indicates the cumulative cost of getting to that point, similar to the DTW counterpart $\tilde{\mathbf{C}}$ as defined in Equation (4), but the y -axis is different. The propagation through \mathbf{C} is

$$\mathbf{C}[i, j] = \Lambda(i, j) + \min \begin{cases} \mathbf{C}[i-1, j], \\ \mathbf{C}[i-1, j-1], \\ \mathbf{C}[i, j+1], \end{cases}$$

where

$$\Lambda(i, j) \equiv |\mathbf{g}[i] - \mathbf{f}[i - j + M]|.$$

$\Lambda(i, j)$ returns the Euclidian distance between two samples. The three directions for calculating \mathbf{C} correspond directly to the three directions in DTW as defined in Equation (4). In one step of $\mathbf{g}[k]$, the delay can go down multiple steps, but can only go up one step at a time. Otherwise, the input can go back in time w.r.t. the output. For this system, the condition for Monotonicity and continuity is

$$0 \leq \mathbf{w}[k+1] \leq \mathbf{w}[k] + 1.$$

This foundation accomplishes a couple of things. First of all, the structure fits better with reporting a value-offset and time-offset for each output sample and also helps with intuitive improvements later in this paper. Secondly, the search space

does not scale quadratically with the signal length as it does in DTW. Limiting the search space reduces the memory requirements and accelerates the algorithm.

With the new foundation in place, we can now easily solve the problem where the start and end forcibly have zero delay. The first column of \mathbf{C} is initialized as $\mathbf{C}(0, *) = [0]^M$. Every starting delay is equally expensive. To remove the ending artefact, we let the last sample of ETO be chosen as the cheapest option, so that

$$\mathbf{C}(N-1, \text{ETO}[N-1]) \leq \mathbf{C}(N-1, j), \quad \forall j \in \mathbb{N}_{<M}$$

B. Introducing penalties for Delay Adjustments

In Section III-B2, we discuss the problem that delay adjustments are largely unpunished. In practice, this means that DTW produces the least possible Euclidean distance, but the delay estimation, indicated with the warp path, is all over the place. For DTW, this is fine, as the Euclidean distance is the only thing that counts to the output, but it is not the case for ETVO.

First, let us define what a delay adjustment is in the context of ETVO; it is a change in estimated delay by a magnitude of time. If multiple changes of the same type happen consecutively, we view that as a single change with a larger magnitude. Recall that the diagonal arrow and down arrow represent an increase and decrease in delay respectively. The dark grey squares in Figure 5 indicate this.

We introduce two penalties to every delay adjustment: P_{fixed} and P_{prop} , that correspond to a penalty that is fixed and proportional to the delay adjustment respectively. These penalties reduce the quantity and magnitude of delay adjustments. Specifically the addition of P_{fixed} makes the algorithm more complicated. Without that penalty, only three places have to be compared, but with the addition of P_{fixed} , that number increases to M . First, the best candidate for each of the three directions is calculated as shown in Equation (6)-(8) and is illustrated in Figure 5.

$$C_{\rightarrow}[i, j] = \mathbf{C}[i-1, j] \quad (6)$$

$$C_{\downarrow}[i, j] = \min_{k \in \mathbb{N}^+} \left\{ \mathbf{C}[i, j+k] + \sum_{l=1}^{k-1} \Lambda(i, j+l) + kP_{\text{prop}} + P_{\text{fixed}} \right\} \quad (7)$$

$$C_{\nearrow}[i, j] = \min_{k \in \mathbb{N}^+} \left\{ \mathbf{C}[i-k, j-k] + \sum_{l=1}^{k-1} \Lambda(i-l, j-l) + kP_{\text{prop}} + P_{\text{fixed}} \right\}. \quad (8)$$

By picking the smallest of these minima, every cell in \mathbf{C} is

$$\mathbf{C}[i, j] = \Lambda(i, j) + \min \{ C_{\rightarrow}[i, j], C_{\downarrow}[i, j], C_{\nearrow}[i, j] \}.$$

P_{fixed} affects the number of delay adjustments, and P_{prop} affects the magnitude of each adjustment. Together, these penalties suppress the delay adjustments estimated by the algorithm.

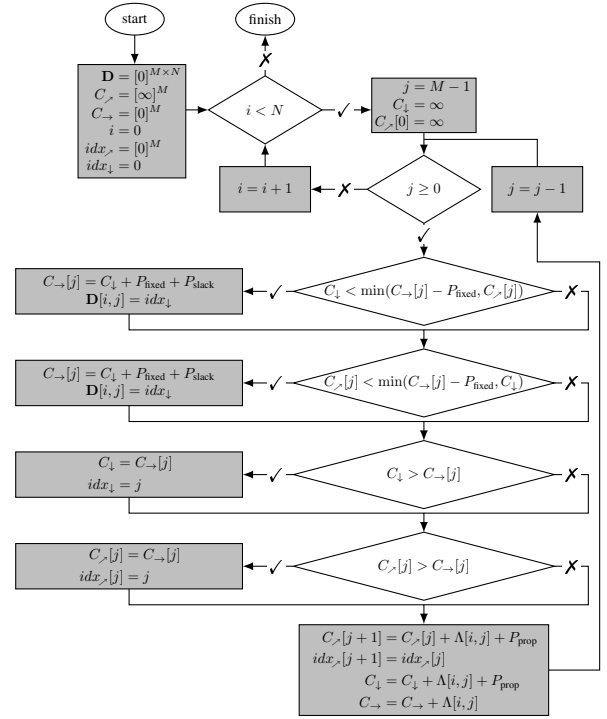


Fig. 6. Flowchart of the algorithm that finds the optimal way of traversing the delay, given the constraints specified for ETO.

C. Improving the timing of delay adjustments

In Section III-B3, we discuss how DTW pursues a minimal solution for the Euclidean distance. In this pursuit, adjustments in delay don't align with the events that justify these changes. Not only is it harder to diagnose a problem, it also makes the algorithm less accurate. The effective time-offset should not change for an event that lies in the future. However for DTW, adjustments can happen at unpredictable moments, often much earlier than the time of the event. The two penalties added in Section IV-B reduce the amount and size of the adjustments, but they do not address this timing issue.

We propose to add slack, where adjustments in time are postponed until the slack value is breached. A penalty P_{slack} acts on top of the other penalties for every delay adjustment, but is only added after an adjustment is made. The effect of P_{slack} is that a delay adjustment is postponed if a change at a later point costs less than the slack value. With the addition of P_{slack} , \mathbf{C} is now

$$\mathbf{C}[i, j] = \Lambda(i, j) + \begin{cases} C_{\rightarrow}[i, j] & \text{if } C_{\rightarrow}[i, j] < \min \{ C_{\downarrow}[i, j], C_{\nearrow}[i, j] \}, \\ C_{\downarrow}[i, j] + P_{\text{slack}} & \text{if } C_{\downarrow}[i, j] < \min \{ C_{\rightarrow}[i, j], C_{\nearrow}[i, j] \}, \\ C_{\nearrow}[i, j] + P_{\text{slack}} & \text{otherwise} \end{cases}$$

The addition of P_{slack} increases the likelihood that the delay adjustments match the events that cause them. This effect makes ETO significantly more realistic and useful for diagnosis.

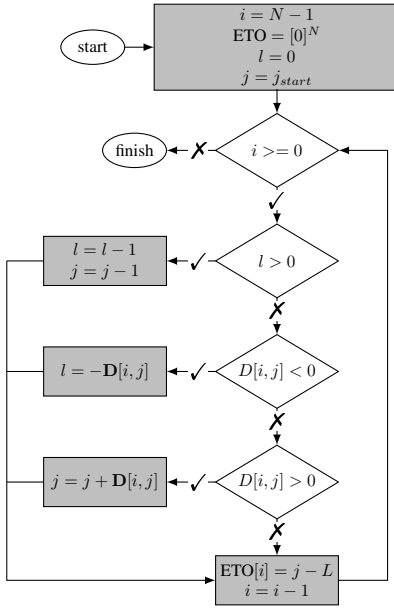


Fig. 7. Flowchart of the backtracking algorithm used to extract the ETO from direction matrix \mathbf{D} .

D. Defining Effective Value-Offset

When using DTW, the remaining distances for every step in the warp sum up to a single number that reports how different the two signals are. We choose to make the value-offset a time-series. A time-series gives more fine-grained information on how different moments in time contribute to the value-offset. Every sample of $EVO[n]$ indicates the cumulative amount of distance from all samples of $g[n]$ compared to the corresponding sample in $f[n]$, excluding penalties. When the delay goes up or stays the same, only one sample of $g[n]$ is compared to $f[n]$, but when the delay goes down, there can be multiple. A description for every element of $EVO[n]$ is given by

$$EVO[i] = \begin{cases} \sum_{l=EVO[k+1]}^{ETO[k]} \Lambda(i, l) & \text{if } ETO[i] > ETO[i+1], \\ \Lambda(i, ETO[i]) & \text{otherwise.} \end{cases}$$

Because of this way of defining $EVO[n]$, there are spikes in value-offset every time the delay goes down by a large amount.

E. Computational optimization's

Besides a mathematical framework for ETO and EVO, we also provide an efficient way of calculating both. Due to the effects of P_{fixed} , there is a larger scope of variables to consider when finding the optimal path. Instead of the three adjacent locations, one has to consider a total of M entries. Besides considering multiple entries, when backtracking to retrieve the delay, one has to consider how many steps were taken. To store that information, we propose a direction matrix $\mathbf{D} \subset \mathbb{Z}^{M \times N}$. The number stored in $\mathbf{D}(k, i)$ indicates that the next point is at $i + \mathbf{D}(k, i)$. Because the direction is stored, there is no need to store \mathbf{C} entirely. There are three directions to consider: up, down, and forward. Each direction has one optimal source from which to go. By remembering only the

optimal continuations in each stage of the algorithm, we only need to store a value and index $C_{\downarrow} \subset \mathbb{R}$ and $idx_{\downarrow} \subset \mathbb{N}$ for downward propagation, arrays $C_{\uparrow} \subset \mathbb{R}^M$ and $idx_{\uparrow} \subset \mathbb{N}^M$ for upward propagation, and array $C_{\rightarrow} \subset \mathbb{R}^M$ for forward propagation. The resulting algorithm for populating \mathbf{D} is illustrated with a flow chart in Figure 6.

The backtracking algorithm needs to account for the multiple steps it can take. The calculation method matches how \mathbf{C} was populated. Figure 7 shows a flow chart of the backtracking algorithm. The complexity of the algorithm for populating \mathbf{D} is determined by two *for loops*. One of the *for loops* is looping through a fixed range M , that does not scale with signal length. Therefore the complexity is $\mathcal{O}(N)$. The complexity of the backtracking algorithm is bound by a single *for loop*, so the upper bound on the combined set is also $\mathcal{O}(N)$.

F. Tuning the penalty values

For DTW, there is only one source of error that counts: Euclidean distance. For ETVO there are also three penalties to consider: P_{prop} , P_{fixed} , and P_{slack} . These penalties should be weighted properly to balance them against the Euclidean distance. P_{prop} should be by far the largest source of penalties during operation. In order to accurately choose how to tune this penalty, we have to state how we rate time noise against value noise. One perspective is to consider time noise to be a source of value noise too. The amount of value noise is linear to the velocity. We suggest to use the specified maximum velocity of the application so that $P_{prop} = t_{sample} \dot{x}_{max}$. However, tuning P_{prop} manually can help to strengthen the understanding of the system behavior.

P_{fixed} suppresses unrealistic optimization and micro-adjustments. In practice, we found that a value of $P_{fixed} = 2P_{prop}$ yields good results. P_{slack} effectively cleans up the signal and makes the timing more accurate, but it only works if P_{slack} is by far the least significant. We found that $P_{slack} \leq P_{prop}$ yields good results. We believe a more sophisticated method or mathematical backing to tune the penalties is possible in the future.

V. EXPERIMENTAL SETUP

To extensively validate our proposed metric, we develop a realistic TI testbed, where a human user can interact with a remotely rendered virtual environment (VE) over a network. We consider a recently proposed testbed for simulating TI interaction (Section V-A). This testbed lacks a network and is therefore not suited for mimicking TI interactions. Hence we carry out significant refinements to realize a networked TI testbed that is fast enough to provide a comfortable TI experience (see Section V-B).

A. Standard TI testbed

The standard TI testbed proposed recently by Bhardwaj et al., simulates a TI session by having the human user interact with a Virtual Environment (VE) in slave domain via haptic and visual feedback [24]. The master domain transmits position information of the haptic device sampling rate of 1 KHz to the slave domain. The resulting calculated force is

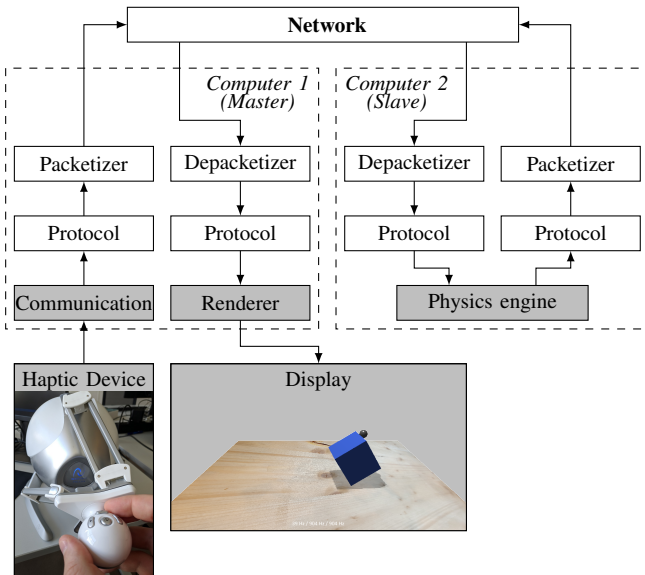


Fig. 8. Schematic overview of our measurement setup. The components present in the reference setup of Bhardwaj et al. highlighted in gray [24].

sent back to the master domain along with the visual rendering of VE. A schematic overview of this setup are indicated as the gray blocks in Figure 8. In this figure, both master and slave domains are collocated for ease of experimentation. The haptic device used in this setup is a Novint Falcon [25]. Force calculation and rendering in the VE is implemented using Chai3D [26].

B. Networked TI testbed

We extend the testbed by decoupling the master and slave domains (each consisting of a workstation) across a network. Therefore, (i) the VE needs to be rendered on a separate workstation, and (ii) the two workstations are connected via a physical network. The local simulation is split into a renderer at the the master domain and a physics engine at the slave domain. The physics engine translates force into movement and sends that as feedback. The real-network conditions are emulated using Netem on a separate workstation running Ubuntu 18.04, that acts as a via between master and slave [27]. Netem can emulate network parameters such as latency, jitter, and packet losses. An schematic overview of the entire system is shown in Figure 8.

To emulate real network conditions, we use the Gilbert-Elliott model to handle packet loss, which is known to closely mimic real network behavior [28]. For delay jitter, We use a high correlation factor of 90% between latency of the packets. We specify the configured parameters of the loss model, average latency, jitter, and the algorithm parameters P_{prop} , P_{fixed} , and P_{slack} in Section V as and when required.

VI. PERFORMANCE ANALYSIS

We conduct rigorous experimentation to comprehensively evaluate our metrics using the networked TI testbed. For the sake of simplicity, we consider only one axis of the position

signal corresponding to the haptic device. Henceforth, we will refer to that axis signal as input. We begin by presenting a case that neatly demonstrates how inconsistent inferences can be drawn by the existing metrics. Thereby demonstrating how none of the existing metrics suffice. Next, we compare the performances of DTW and ETVO. We formulate several scenarios which enables easy understanding of the working of ETVO. It is worth mentioning that the performance gains of ETVO over other schemes holds true in any setting.

A. Contradicting inferences between QoE and QoS metrics

We choose HPW-PSNR [10] as the QoE metric, and latency as the QoS metric. Note that similar scenarios can be observed for other combinations of QoE and QoS metrics. Using our testbed, We record the position trace of the haptic device during the TI interaction. In order to visualize how two different TI systems could alter the input, we add a latency of 15 ms and 50 ms to the input signal. For all practical purposes, this is equivalent to the latency induced by the TI systems. Note that for the sake of brevity, we are only showing a small fragment of the complete signal.

As per the latency, it is quite obvious that the former TI system outperforms the latter since it introduces lower latency. Now, we measure the HPW-PSNR of the two output signals with respect to the input signal. We observe that the both systems have an equal HPW-PSNR of 9.21. This is due to the fact that adding a static latency to a signal makes no difference to the PSNR. Going by HPW-PSNR, the performances of the two systems are identical which completely contradicts the inference drawn on the basis of latency. Hence, existing metrics can often lead to ambiguous situations, thereby reinforcing the need for the proposed quantitative metrics that can better represent the TI system performance.

B. Comparing DTW and ETVO

To illustrate the differences in behavior between DTW and ETVO, we picked four fragments of time each corresponding to a different signal.

1) *Context-sensitivity*: We start by gauging the sensitivity of each of the schemes to the signal context. For this experiment, we set the following configuration: **[average lat., jitter, P_{prop} , P_{fixed}] = [15 ms, 10 ms, 0.01, 0.005]**. The first fragment (leftmost column) in Figure 9 corresponds to this setup. It can be observed that when the velocity is high (extremes of the plot), DTW shows vigorous fluctuations in time-offset estimation. On the other hand, ETVO sensibly changes its estimation of ETO exhibiting resilience to noise component in the signal. When the velocity is low in the middle, ETVO being context-aware stops adjusting the ETO since there is negligible improvement in EVO. DTW however, does not care about how minor changes and keeps constantly adjusting the time-offset, irrespective of the context. NPS stands for No P_{slack} , where one can see that a change in delay is randomly made in them middle of the quiet period (as indicated with 1), while the ETO with P_{slack} postpones that decision to when something happens again. Note that the EVO and DTW signal are reasonably similar, despite the significantly higher number

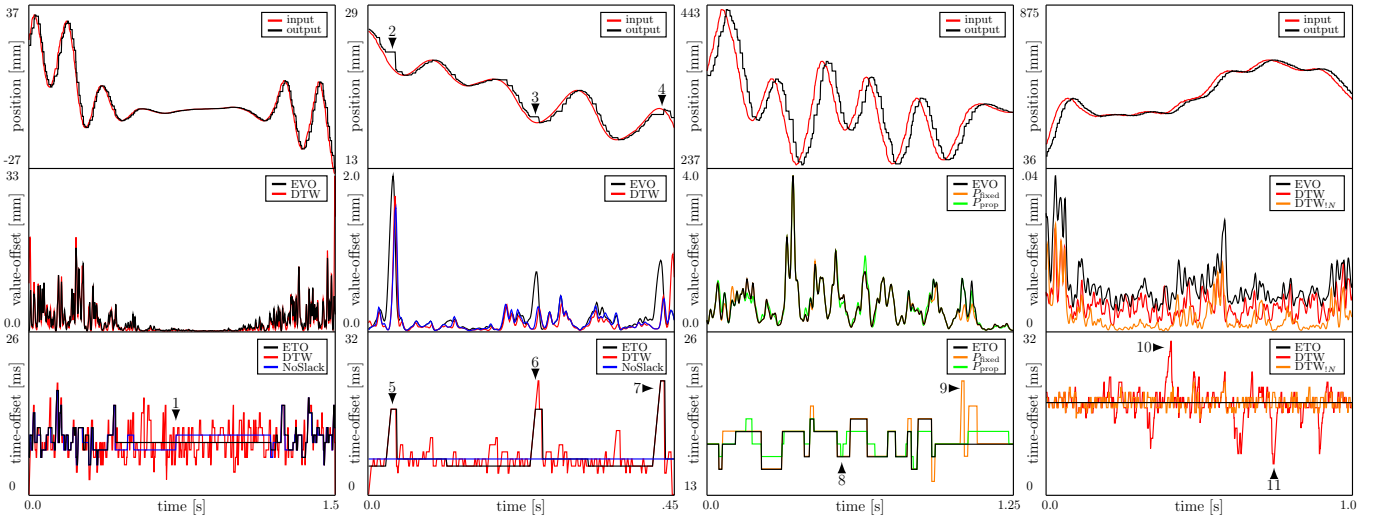


Fig. 9. This plot shows four fragments of four different measurements with the setup under varying circumstances

of delay adjustments performed by DTW. DTW concludes that the delay fluctuates wildly all the time, while ETVO concludes that the effects are only noticeable when there is high velocity. ETVO reasonably concludes that a higher update rate is desired when more is happening. This example shows how ETVO makes evaluations that are context-aware.

2) *Lack of updates*: In this scenario, we investigate the performance in presence of fewer haptic updates. We emulate this scenario through two processes: perceptual deadband [29] and packet losses. This enables us to evaluate the performance when the value-offset is considerable. We choose a deadband of 5% and bursty loss following the Gilbert-Elliott model with parameters $p = 5\%$ and $r = 50\%$, as prescribed in [30]. For this experiment, we set the following configuration: **[average lat., jitter, P_{prop} , P_{fixed}] = [0 ms, 0 ms, 0.005, 0.005]**. The second column of Figure 9 corresponds to this scenario.

It can be clearly seen that the output signal is subject to noticeable jitter due to the combined effect of packet loss and deadband. However, there are three specific instances (indicated by labels 2-4) where the combined effect of deadband and bursty losses prominently results in no change in output signal. In this case, DTW chooses to relentlessly adjust the time-offset as the deadband and losses are slightly degrading the signal. ETVO, however, remains robust to the jitter for the most part and sits at the average delay. But in cases where the effect is prominent, ETO is adjusted as indicated with labels 5-7. The value-offset is smoothed with a Gaussian distribution for the purpose of visual clarity. As one would expect, EVO is slightly higher than value-offset in DTW. Although each of the schemes perform their corresponding tasks accurately, the behavior that is most favorable for TI applications is exhibited by ETVO. Especially considering that time variations are considered to be extremely detrimental to the session quality.

3) *Impact of P_{prop} and P_{fixed}* : The third column in Figure 9 uses the same network settings as specified in Section VI-B1. We consider three settings for algorithm parameters:

- (i) $[P_{prop}, P_{fixed}] = [0.025, 0.05]$ (corresponds to black curve),
- (ii) $[P_{prop}, P_{fixed}] = [0.05, 0]$ (corresponds to amber curve), and
- (iii) $[P_{prop}, P_{fixed}] = [0, 0.1]$ (corresponds to green curve).

This part shows the distinct effects of using only P_{prop} or P_{fixed} on the metrics, and the necessity of considering both. Label 7 indicates an event where the ETO with $P_{fixed} = 0$ adjusts in multiple small steps. In this case, there is no difference in extra cost associated with using multiple steps, causing the amount of adjustments to increase. Label 8 indicates an event where the ETO with $P_{prop} = 0$ causes a large step changes but limited in the number of steps. In this case, there is no extra cost associated with how much the ETO changes, giving rise to ETO adjustments that are unreasonably large. The signal that has both components has a similar performance in EVO, but a significantly less cluttered ETO.

4) *Effect of noise*: The last column in Figure 9 corresponds to the following configuration: **[average lat., jitter, P_{prop} , P_{fixed} , P_{slack}] = [15 ms, 1 ms, 0.005, 0.01, 0.005]** Additionally, we introduce AWGN with an SNR of 70 dB. This fragment shows the effect that high frequency noise has on DTW and ETVO. Both DTW and EVO are plotted with the noise added, while DTW_{1N} , is a version of DTW without the added AWGN. High frequency noise is a good example of a common addition to a signal that DTW cannot deal with properly. Note that ETVO outperforms the best case DTW i.e. DTW_{1N} , demonstrating its noise resilience. Further, one can also notice the vulnerability of DTW to even a marginal amount of noise causing time-offset to fluctuate vigorously.

C. Long-term average behavior

From previous subsections we demonstrate the behavior of ETVO with respect to DTW in a short timescale. Most notably we demonstrate a reduction in delay adjustments of several orders of magnitude. This reduction is essential to make the algorithm eligible for use in TI, as time jitter is considered to be one of the most detrimental properties. In this section we demonstrate that the proposed measure behaves consistently

TABLE I
COMPARISON BETWEEN ETVO AND DTW FOR LONG TERM
PERFORMANCE

Time jitter	5 ms	10 ms	25 ms	50 ms
RMSE				
ETVO	$2.5 \cdot 10^{-3}$	$3.4 \cdot 10^{-3}$	$4.9 \cdot 10^{-3}$	$9.8 \cdot 10^{-3}$
DTW	$1.8 \cdot 10^{-3}$	$3.1 \cdot 10^{-3}$	$2.8 \cdot 10^{-3}$	$9.6 \cdot 10^{-3}$
Constant delay	$2.8 \cdot 10^{-3}$	$4.5 \cdot 10^{-3}$	$7.5 \cdot 10^{-3}$	$1.5 \cdot 10^{-2}$
Time noise				
ETVO	$4.8 \cdot 10^{-3}$	$2.7 \cdot 10^{-2}$	$8.1 \cdot 10^{-2}$	0.183
DTW	0.30	0.37	0.45	0.51
Constant delay	0	0	0	0
Probability of time adjustment				
ETVO	$5.7 \cdot 10^{-3}$	$2.0 \cdot 10^{-2}$	$5.3 \cdot 10^{-2}$	$9.7 \cdot 10^{-2}$
DTW	0.26	0.24	0.28	0.27
Constant delay	0	0	0	0

throughout longer durations. We conduct six runs of experiments with durations larger than 30s and time jitter being 5 ms, 10 ms, 25 ms, and 50 ms. We compare three methods: DTW, ETVO, and a scenario that has a constant delay at the delay that yields the least RMSE. We compare these methods for each experiment on RMSE, Time noise and Probability of time adjustment. Here, time noise is the cumulative amount of adjusted time normalized over the duration of the sequence. Probability of time adjustment represents the probability of the delay being adjusted by the method for a single step. The findings shown in Table I reveal that for these values, DTW has little correlation with the time jitter that was added. The amount of time noise has only some correlation to the jitter, and the average number of changes is consistent for each of the experiments, where DTW has a 25% probability each step to make an adjustment. Also the RMSE reported by DTW is only loosely correlated to the actual noise that is present in the system. DTW is so aggressive with optimizing the match that it under reports the effect of time noise. ETVO shows strong correlation between noise present and the reported values in each category. The RMSE steadily rises when the jitter goes up, it reports gradually more time noise, and the probability of adjustments goes up significantly as the actual delay varies more.

Between all of the four experiments, ETVO exchanges 34% more RMSE for $62.5\times$ less time noise in the 5 ms experiment; 23% more RMSE for $11.1\times$ less time noise in the 10 ms experiment; 10% more RMSE for $5.6\times$ less time noise in the 25 ms experiment; 2.4% less RMSE for $2.8\times$ less time noise in the 50 ms experiment. Note that ETVO can have a lower RMSE than DTW due to the boundary conditions for DTW. For the sake of comparison, we include an option where the delay can only be changed once at the start. This is equivalent to setting the $P_{\text{fixed}} = \infty$. For this method the RMSE does rise substantially.

VII. CONCLUSION AND FUTURE WORK

As the field of Tactile Internet (TI) is advancing fast, there is a strong need for quantifying performance sessions

objectively. In this paper, we first presented the severe shortcomings of the state of the art in TI performance metrics, and that they are unsuitable for proper characterization of TI sessions and systems. To overcome these limitations, we started at the Dynamic Time Warping (DTW) algorithm, and proposed two novel concepts: Effective Time-Offset (ETO) and Effective Value-Offset (EVO) that enable representation of TI performance at a fine scale. We provided a concrete mathematical framework for these concepts. Through rigorous experiments using a haptic tool, we demonstrated their salient features. We demonstrate how ETO and EVO are a context-aware and noise-resilient estimation of similarity between the input and output sequences. Further, we demonstrated that our proposed scheme significantly outperforms the popular DTW algorithm. Furthermore, we demonstrated that state of the art in performance metrics is insufficient for complete characterization of TI systems. We demonstrated the improved decision making with fine-grained examples, and a long-term average behavior showing up to $62.5\times$ less time noise for up to 34% increased RMSE.

Objective metrics for measuring subjective quality will enable significant improvements in several dimensions of TI. While the current work looks at an offline session, we intend to solve the non-trivial problems of measuring objectively in real-time in the near future. The complete implementation code will be made available as an open source.

REFERENCES

- [1] G. P. Fettweis, "The tactile internet: Applications and challenges," *IEEE Vehicular Technology Magazine*, vol. 9, no. 1, pp. 64–70, 2014.
- [2] C. Basdogan, C.-H. Ho, M. A. Srinivasan, and M. Slater, "An experimental study on the role of touch in shared virtual environments," *ACM Transactions on Computer-Human Interaction (TOCHI)*, vol. 7, no. 4, pp. 443–460, 2000.
- [3] A. Aijaz and M. Sooriyabandara, "The tactile internet for industries: A review," *Proceedings of the IEEE*, vol. 107, no. 2, pp. 414–435, 2018.
- [4] D. A. Lawrence, "Stability and transparency in bilateral teleoperation," *IEEE transactions on robotics and automation*, vol. 9, no. 5, pp. 624–637, 1993.
- [5] V. Millnert, J. Eker, and E. Bini, "Achieving predictable and low end-to-end latency for a network of smart services," in *2018 IEEE Global Communications Conference (GLOBECOM)*. IEEE, 2018, pp. 1–7.
- [6] S. Samarakoon, M. Bennis, W. Saad, and M. Debbah, "Federated learning for ultra-reliable low-latency v2v communications," in *2018 IEEE Global Communications Conference (GLOBECOM)*. IEEE, 2018, pp. 1–7.
- [7] F. Gringoli, R. Klose, M. Hollick, and N. Ali, "Making wi-fi fit for the tactile internet: Low-latency wi-fi flooding using concurrent transmissions," in *2018 IEEE International Conference on Communications Workshops (ICC Workshops)*. IEEE, 2018, pp. 1–6.
- [8] Z. Yuan, S. Chen, G. Ghinea, and G.-M. Muntean, "User quality of experience of mulsemmedia applications," *ACM Transactions on Multimedia Computing, Communications, and Applications (TOMM)*, vol. 11, no. 1s, p. 15, 2014.
- [9] R. Chaudhari, E. Steinbach, and S. Hirche, "Towards an objective quality evaluation framework for haptic data reduction," in *2011 IEEE World Haptics Conference*. IEEE, 2011, pp. 539–544.
- [10] N. Sakr, N. Georganas, and J. Zhao, "A perceptual quality metric for haptic signals," in *2007 IEEE International Workshop on Haptic, Audio and Visual Environments and Games*. IEEE, 2007, pp. 27–32.
- [11] P. Hintenseer, E. Steinbach, and S. Chaudhuri, "Perception-based compression of haptic data streams using kalman filters," in *2006 IEEE International Conference on Acoustics Speech and Signal Processing Proceedings*, vol. 5, May 2006, pp. V–V.

- [12] A. Hamam, M. Eid, A. El Saddik, and N. D. Georganas, "A quality of experience model for haptic user interfaces," in *Proceedings of the 2008 Ambi-Sys workshop on Haptic user interfaces in ambient media systems*. ICST, 2008, p. 1.
- [13] M. Eid, J. Cha, and A. El Saddik, "Admux: An adaptive multiplexer for haptic-audio-visual data communication," *IEEE Transactions on Instrumentation and Measurement*, vol. 60, no. 1, pp. 21–31, 2010.
- [14] B. Cizmeci, X. Xu, R. Chaudhari, C. Bachhuber, N. Alt, and E. Steinbach, "A multiplexing scheme for multimodal teleoperation," *ACM Trans. Multimedia Comput. Commun. Appl.*, vol. 13, no. 2, pp. 21:1–21:28, Apr. 2017. [Online]. Available: <http://doi.acm.org/10.1145/3063594>
- [15] V. Gokhale, J. Nair, and S. Chaudhuri, "Congestion control for network-aware telehaptic communication," *ACM Trans. Multimedia Comput. Commun. Appl.*, vol. 13, no. 2, pp. 17:1–17:26, Mar. 2017. [Online]. Available: <http://doi.acm.org/10.1145/3052821>
- [16] L. R. Rabiner and B. Gold, "Theory and application of digital signal processing," *Englewood Cliffs, NJ, Prentice-Hall, Inc., 1975. 777 p.*, 1975.
- [17] H. Sakoe and S. Chiba, "Dynamic programming algorithm optimization for spoken word recognition," *IEEE Transactions on Acoustics, Speech, and Signal Processing*, vol. 26, no. 1, pp. 43–49, 1978.
- [18] S. Salvador and P. Chan, "Toward accurate dynamic time warping in linear time and space," *Intelligent Data Analysis*, vol. 11, no. 5, pp. 561–580, 2007.
- [19] G. Al-Naymat, S. Chawla, and J. Taheri, "Sparsedtw: A novel approach to speed up dynamic time warping," in *Proceedings of the Eighth Australasian Data Mining Conference-Volume 101*. Australian Computer Society, Inc., 2009, pp. 117–127.
- [20] D. F. Silva and G. E. Batista, "Speeding up all-pairwise dynamic time warping matrix calculation," in *Proceedings of the 2016 SIAM International Conference on Data Mining*. SIAM, 2016, pp. 837–845.
- [21] L. Chen, M. T. Özsu, and V. Oria, "Robust and fast similarity search for moving object trajectories," in *Proceedings of the 2005 ACM SIGMOD international conference on Management of data*. ACM, 2005, pp. 491–502.
- [22] L. Chen and R. Ng, "On the marriage of lp-norms and edit distance," in *Proceedings of the Thirtieth international conference on Very large data bases-Volume 30*. VLDB Endowment, 2004, pp. 792–803.
- [23] M. Vlachos, D. Gunopoulos, and G. Kollios, "Discovering similar multidimensional trajectories," in *icde*. IEEE, 2002, p. 0673.
- [24] A. Bhardwaj, B. Cizmeci, E. Steinbach, Q. Liu, M. Eid, A. E. Saddik, R. Kundu, X. Liu, O. Holland, M. A. Luden, S. Oteafy, and V. Prasad, "A Candidate Hardware and Software Reference Setup for Kinesthetic Codec Standardization," in *2017 IEEE International Symposium on Haptic, Audio and Visual Environments and Games (HAVE)*, 2017, pp. 53–58.
- [25] (2015) Novint falcon - product page. [Online]. Available: <https://web.archive.org/web/20150215032400/http://www.novint.com/index.php/products/novintfalcon>
- [26] (2019) Chai3d - features. [Online]. Available: <https://www.chai3d.org/concept/features>
- [27] (2019) networking:netem [wiki]. [Online]. Available: <https://wiki.linuxfoundation.org/networking/netem>
- [28] G. Haßlinger and O. Hohlfeld, "The gilbert-elliott model for packet loss in real time services on the internet," in *14th GI/ITG Conference-Measurement, Modelling and Evaluation of Computer and Communication Systems*. VDE, 2008, pp. 1–15.
- [29] I. Vittorias, J. Kammerl, S. Hirche, and E. Steinbach, "Perceptual coding of haptic data in time-delayed teleoperation," in *World Haptics 2009-Third Joint EuroHaptics conference and Symposium on Haptic Interfaces for Virtual Environment and Teleoperator Systems*. IEEE, 2009, pp. 208–213.
- [30] M. Ellis, D. P. Pezaros, T. Kypraios, and C. Perkins, "A two-level markov model for packet loss in udp/ip-based real-time video applications targeting residential users," *Computer Networks*, vol. 70, pp. 384–399, 2014.